

Microwave-assisted sol-gel synthesis and optical property of TiO₂ thin film

HUAMING YANG*, XIANGCHAO ZHANG, QIUFEN TAO, AIDONG TANG^A

Department of Inorganic Materials, School of Resources Processing and Bioengineering, Central South University, Changsha 410083, China

School of Chemistry and Chemical Engineering, Central South University, Changsha 410083, China

Titanium dioxide (TiO₂) thin film has been successfully synthesized deposited on glass substrates by the sol-gel dip-coating method using microwave heating. The precursor and TiO₂ film were characterized using thermogravimetric and differential scanning calorimetric (TG-DSC), X-ray diffraction (XRD), atomic force microscopy (AFM) and UV-visible (UV-vis) absorption spectra analysis technology. The preparation of the precursor sols and TiO₂ film were described in detail. The XRD result demonstrates that the TiO₂ film is well crystallized and consists of anatase phase only with (101) plane. The morphology of the nanoparticles of TiO₂ thin film is spherical shape with grain size of 68.2 nm in average diameter and the surface of the TiO₂ film is smooth. There is a strong wide UV absorption band around 387 nm for the prepared TiO₂ film. The calculated band gap (E_g) value of the TiO₂ thin film by microwave heating is about 3.4 eV for direct transition and about 3.2 eV for indirect transition, respectively. The microwave heating offers a novel process route in treating thin film for commercial applications.

(Received May 23, 2007; accepted June 27, 2007)

Keywords: Titanium dioxide (TiO₂), Thin films, Microwave heating, Optical property

1. Introduction

Titanium dioxide (TiO₂), a novel inorganic function material with wide bandgap, has recently attracted much attention because it is one of the most prominent materials in the areas of photocatalysis, photovoltaic devices, dye-sensitized solar cells, sensors, batteries and potential tool in cancer treatment due to their excellent optical, electrical, photocatalytic and thermal properties [1-6], for example, transparency to visible light, electronic conductivity, high surface affinity towards certain ligands, and large surface area [1-7]. It is generally accepted that the properties of TiO₂ thin film depend on their microstructure, morphology, porosity and crystallinity. Preparation methods enabling the control of the structural properties are especially desired [7,8].

There are many routes to synthesize TiO₂ thin films to obtain the optimum size and phase of crystalline TiO₂, including sputtering, chemical vapor deposition (CVD), spray pyrolysis, electrodeposition, self-assembly and sol-gel [9-16]. Among these methods, the sol-gel process is one of the most appropriate technologies to prepare thin oxide films. The interest in application of sol-gel method is due to several advantages, such as good homogeneity, ease of composition control, large area coatings, low equipment cost and good photocatalytic properties. However, The TiO₂ film synthesized by sol-gel technique

is typically sintered at 350-550°C for approximately 30-120 min to achieve crystallization to the anatase phase and good connections between the TiO₂ nanoparticles [14-17]. The character of conventional heating is that the materials are heated from the outer part to the inner part, which will lead to inhomogenous distribution of temperature. On the contrast, the mechanism of microwave heating is that both the outer part and the inner part of material are heated simultaneously. As a result, thermal gradients during microwave processing can be avoided and can provide a clean, cost-effective, energy efficient, faster, and convenient method of heating, which results in higher yields and shorter-time reactions [18-19]. Recently, the microwave heating has attracted much interest. This method has been successfully applied for the preparation of a variety of nanosized inorganic materials [18-21].

In this paper, anatase TiO₂ thin film was deposited on glass slides substrates by dip-coating method and was subsequently heated by microwave technique. It gives in detail the preparation of the precursor sols, the film gel precursor was characterized using different method, the morphology, crystallinity and optical properties of the film was examined.

2. Experimental

2.1 Preparation of precursor

The precursor of TiO_2 sol was synthesized by a sol-gel method, using titanium tetrabutoxide ($\text{Ti}(\text{OC}_4\text{H}_9)_4$, TTBO), diethanolamine ($\text{NH}(\text{CH}_2\text{CH}_2\text{OH})_2$, DEA) and anhydrous alcohol ($\text{C}_2\text{H}_5\text{OH}$, EtOH) as starting materials. All reagents were analytical grade and used without further purification. 17.02 ml TTBO and 4.8 ml DEA were mixed with 68.28 ml EtOH, the solution was completely mixed and then stirred under vigorous magnetic agitation for 60 min at room temperature. Afterwards, the mixed solution was added dropwise into another mixture consisting of 0.9 ml deionized water and 10 ml EtOH under roughly stirring to perform hydrolysis. DEA serves as a stabilizer to hinder the hydrolysis of TTBO. The chemical composition of the starting alkoxide solution was TTBO:EtOH: H_2O :DEA = 1:26.5:1:1 in molar ratio. After continuously stirring for 2 h, a yellowish transparent sol of 0.5 mol/l [Ti] in molar concentration was obtained, which was then aged for 48 h and served for film preparation.

2.2 Formation of TiO_2 thin film

TiO_2 thin film was prepared by a dip-coating method. Prior to the coating process, soda-lime-silica glass substrates (microscope slides) with dimension $75\text{mm} \times 25\text{mm} \times 1.5\text{mm}$ were ultrasonically cleaned in potassium dichromate solutions, and rinsed with anhydrous alcohol and deionized water. They were then dried at 100°C in air. The TiO_2 gel film was obtained by dipping the substrate in the precursor solution bath and pulled upwards with a constant speed of 4 cm/min to keep uniform thickness of the film. The substrates coated with gel films were heat-treated for 5 min using a domestic microwave oven (700W, 2.45GHz, Galanz, China) with a four-stub tuner, the microwave power could be varied from 40%(280 W), 66%(462W), 85%(595W) to 100%(700W) of power output. In this paper, High power (700W) was selected to heat the TiO_2 film. The thickness of the TiO_2 film was adjusted by repeating the cycle from withdrawing to heat treatment. The films were coated with six layers. The detailed process is shown in the flow chart (Fig.1).

2.3 Characterization of TiO_2 film

Crystallinity of the TiO_2 film was identified by X-ray diffraction (XRD) using a Rigaku D/max 2550 diffractometer with graphite monochromatized Cu K_α radiation ($\lambda = 1.54056\text{\AA}$). The different patterns were collected at steps of 0.02° in the 2θ range from 10° to 85° . The accelerating voltage and the applied current were 40 kV and 300 mA, respectively. Simultaneous thermogravimetric and differential scanning calorimetric (TG-DSC) analysis of the precursor was carried out using an SDT2960 thermal analysis, the sample was treated in

air from room temperature to 600°C at a rate of $10^\circ\text{C}/\text{min}$ with Al_2O_3 as reference. The surface morphology was observed using a NT-MDT atomic force microscopy (AFM) with silicon probe tapping contact mode. The UV-visible absorption spectra of the sample were performed using a UV-visible spectrophotometer (UV-2450) with a wavelength range of 300–900 nm.

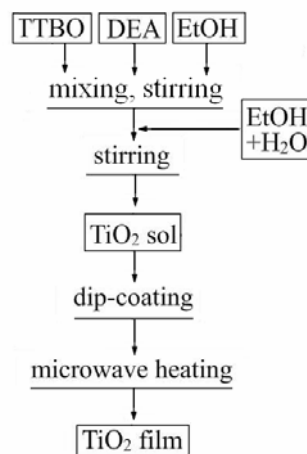


Fig.1. Schematic diagram for preparation TiO_2 film using microwave heating technique

3. Results and discussion

3.1 Thermal analysis

TG-DSC was applied to characterize the film gel precursor to determine the transition process of gel to the target film during heating. Fig. 2 showed the TG-DSC curves of the dry TiO_2 gel powder. It could be found that there were three main stages during the weight loss process of TiO_2 gel from the TG curve. One was the weight loss of about 6% at the temperature from room temperature to 200°C , corresponding to the appearance of an endothermic peak around 100°C in DSC curve and indicating the elimination of the desorption of water and ethanol in the gel. Second stage was the obvious weight loss of 10% from 200°C to 300°C . According to the DSC curve, the endothermic peaks around 275°C is probably due to the combustion decomposition of some organic matters. The third part was from 300°C to 500°C and the weight loss was about 30%, however, it was not evident after 400°C , which possibly resulted from the desorption of the hydroxyl (OH) group on the surface of TiO_2 nanoparticles. It is known that there are two types of surface OH groups, i.e. terminal Ti-OH and bridge Ti(OH)Ti. Dissociation temperatures of these surface OH groups differ from each other, and each temperature also

could be affected by the chemical surroundings. Thus, the decrease in the weight loss was not obvious. In DSC curve, there is an exothermic peak around 325°C resulting from the crystallization of TiO₂ from the amorphous phase to the anatase phase, and another endothermic peak around 510°C is possibly be associated with the phase conversion from anatase to rutile phase.

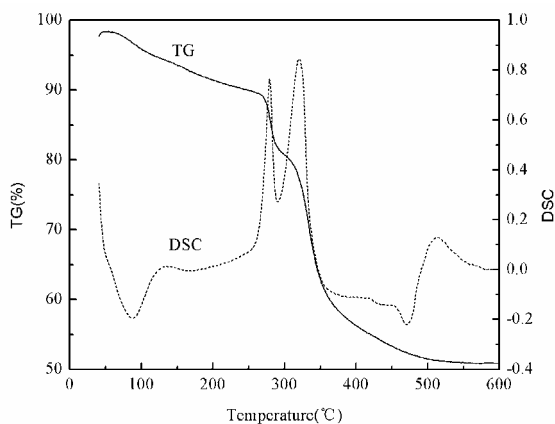


Fig. 2. TG-DSC curves of the dry TiO₂ gel powder.

3.2 XRD analysis

The XRD patterns of the as-synthesized samples have been analyzed to study the phase structure. The thickness of TiO₂ film is so thin that it is difficult to reveal the crystalline structure of TiO₂ film deposited on glass substrate in the diffraction. Therefore, the TiO₂ powders were simultaneously prepared by treating the same dry TiO₂ gel powder for 30 min using microwave heating under the same experimental conditions. Fig. 3 shows the XRD patterns for TiO₂ film and powders prepared by microwave heating.

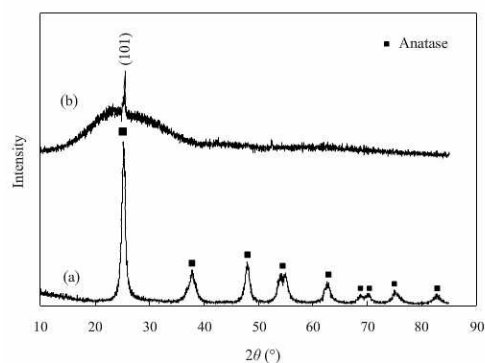


Fig. 3. XRD patterns for (a) TiO₂ powder prepared by microwave heating and (b) TiO₂ film.

In Fig. 3a, all diffraction peaks can be readily indexed to TiO₂ with anatase structure (JCPDS 21-1272). As shown in Fig. 3b, there is a broad hump in the low 2θ region of 15° to 38°, which characterizes an amorphous phase corresponding to the glass substrate. It also has been found that a sharp peak at $2\theta = 25.3^\circ$ superimposed on the broad hump, which clearly indicates the presence of a crystalline phase in addition to the amorphous phase. The XRD results demonstrate that the TiO₂ film is well crystallized and consists of anatase phase only with (101) plane, being in agreement with the XRD results of TiO₂ powders.

3.3 AFM morphology of TiO₂ film

The tapping mode of AFM was used to study the morphologies of TiO₂ film prepared by microwave heating. AFM two- and three-dimensional images of TiO₂ film deposited on glass substrate are shown in Fig. 4. As shown in Fig. 4, the nanoparticles of TiO₂ thin film exhibit spherical shape. The surface of TiO₂ thin film was smooth, with the maximum protuberance about 84.4 nm high and the size of TiO₂ nanoparticles was 68.2 nm in average. The image based root mean square roughness (RMS) for the TiO₂ films is 8.3 nm.

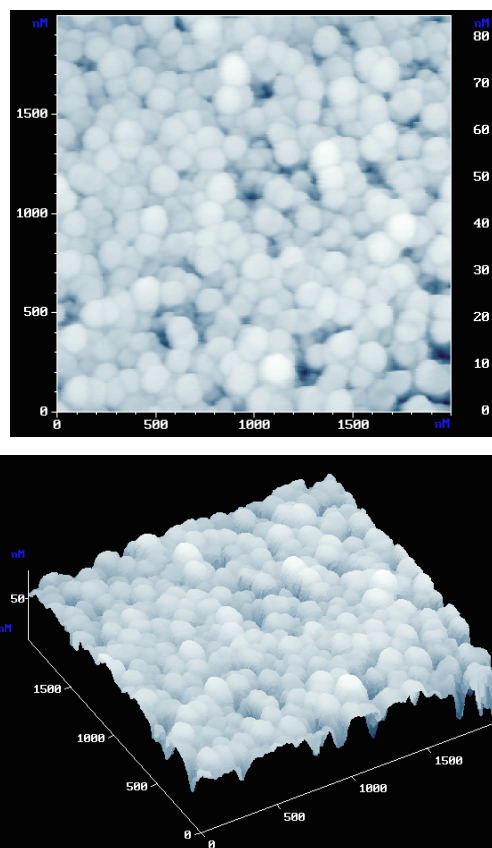


Fig. 4. AFM two- and three-dimensional images of TiO₂ films deposited on glass substrate using microwave heating

3.4 Optical properties

Fig. 5 gives the UV-vis absorption spectra of the six-layer TiO₂ film coated on glass substrate. It can be seen that there is a strong wide UV absorption band (300–387 nm) with a steep edge around 387 nm for the prepared TiO₂ film, but no absorption is observed at wavelengths longer than 387 nm. This indicates that the prepared film could absorb almost all UV lights from 300 to 387 nm, and the wavelength shows less effect on the absorption strength of the lights. This remarkable UV absorption property of the intrinsic TiO₂ provides an important experimental proof for the application of TiO₂ film to UV sensor. In addition, some weak absorption peaks were observed in the visible (vis) light region, which was not caused by the absorption of the TiO₂ film, but arose from the wave interference of the film.

In order to establish the type of band-to-band optical transition in the synthesized TiO₂ film, the absorption data were fitted to following equations for both indirect and direct band-gap transitions [22,23]: $\alpha h\nu = A (h\nu - E_g)^n$, where α is the absorption coefficient (cm⁻¹), $h\nu = 1239.84/\lambda$ is the energy of excitation (eV), λ is the wavelength (nm), A is a constant which does not depend on photoenergy, $n=2$ for indirect transmission and $n=1/2$ for direct transmission.

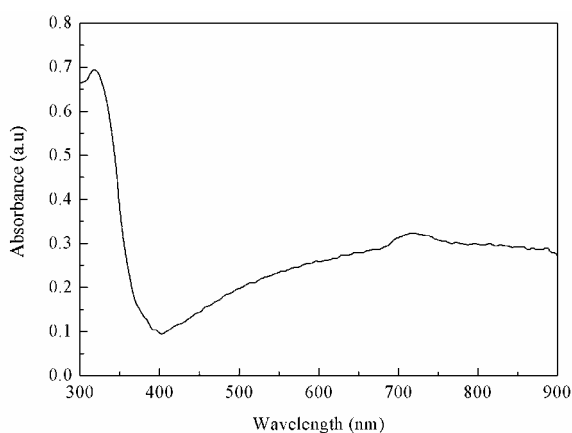


Fig. 5. UV-vis absorption spectra of TiO₂ film deposited on glass substrate using microwave heating.

A quantitative evaluation of the band gap energy (E_g) can be performed by plotting $(\alpha h\nu)^{1/n}$ versus $h\nu$ and extrapolated from linear part of the curve as shown in the Fig. 6. Fig. 6a show the $(\alpha h\nu)^2$ versus $h\nu$ for a direct transition and Fig. 6b show the $(\alpha h\nu)^{1/2}$ versus $h\nu$ for an indirect transition, respectively. The calculated band gap (E_g) value of the anatase TiO₂ thin film by microwave heating is about 3.4 eV for direct transition and about 3.2 eV for indirect transition, which agrees with the results that the band gap energy of sol-gel derived TiO₂ film using microwave irradiation for indirect transition is smaller than that for direct transition[24].

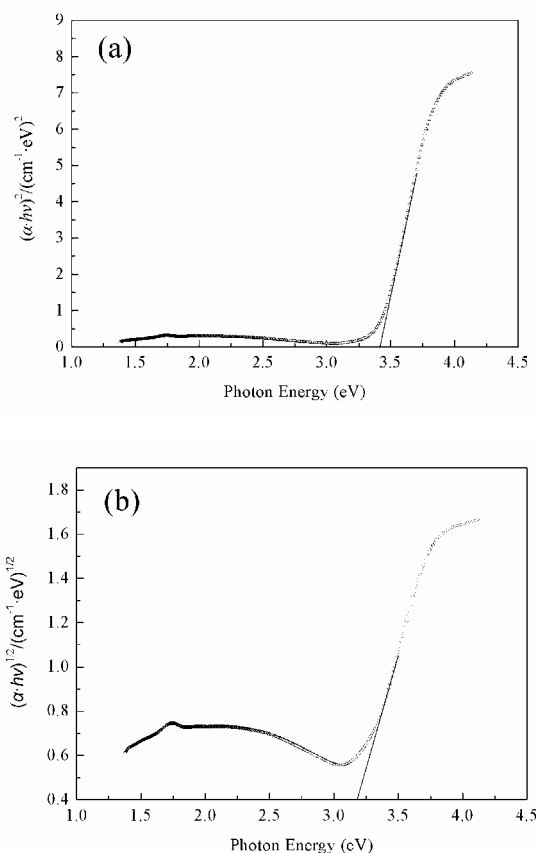


Fig. 6. Plots of (a) $(\alpha h\nu)^2$ versus $h\nu$ for direct transition and (b) $(\alpha h\nu)^{1/2}$ versus $h\nu$ for indirect transition of anatase TiO₂ film deposited on glass substrate using microwave heating.

4. Conclusions

Titanium dioxide (TiO₂) thin film has been successfully synthesized using microwave heating deposited on glass substrates by the sol-gel dip-coating method. Microwave processing may allow a reduction in the required temperature and time for the heat treatment. The technique offers a novel process route to prepare film for commercial applications. The results demonstrate that the TiO₂ film is well crystallized with smooth morphology and spherical shape with grain size of 68.2 nm. There is a strong wide UV absorption band around 387 nm for the prepared TiO₂ film. The calculated band gap (E_g) value of the TiO₂ thin film is about 3.4 eV for direct transition and about 3.2 eV for indirect transition, respectively.

Acknowledgements

This work was supported by the Program for New Century Excellent Talents in University (NCET-05-0695) and the Program for New Century 121 Excellent Talents in Hunan Province (No. 05-030119) and the Postgraduate Educational Innovation Engineering of Central South University (No.1343-76236).

References

- [1] S.Y. Chae, M.K. Park, S.K. Lee, T.Y. Kim, S.K. Kim, W.I. Lee. *Chem. Mater.*, **15**, 3326 (2003)
- [2] J.G. Doh, J.S. Hong, R. Vittal, M.G. Kang, N.G. Park and K.J. Kim. *Chem. Mater.* **16**, 493 (2004).
- [3] D. Zhang, T. Yoshida, T. Oekermann, K. Furuta, H. Minoura. *Adv. Funct. Mater.* **16**, 1228 (2006).
- [4] A. Rothschild, F. Edelman, Y. Komem, F. Cosandey, *Sensor. Actuat B-Chem.* **67**, 282 (2000).
- [5] K. Shankar, K.C. Tep, G.K. Mor, C. A. Grimes. *J. Phys. D: Appl. Phys.* **39**, 2361 (2006).
- [6] U. Diebold, *Appl. Phys. A.* **76**, 681 (2003).
- [7] S.Y. Choi, M. Mamak, S. Speakman, N. Chopra, G.A. Ozin. *Small* **1**(2), 226 (2005).
- [8] D.V. Bavykin, J.M. Friedrich, F.C. Walsh. *Adv. Mater.* **18**, 2807 (2006).
- [9] R. Wang, K. Hashimoto, A. Fujishima, M. CHikuni, E. Kojima, A. Kitamura, M. Shimohigoshi, T. Watanabe. *Adv. Mater.* **10**(2), 135 (1998).
- [10] Jung-Chul Lee, Kyung-Soo Park, Tae-Geun Kim. *Nanotechnology*, **17**, 4317 (2006).
- [11] I. Oja, A. Mere, M. Krunk, R. Nisumaa, C. H. Solterbeck, M. E. Souni. *Thin Solid Films* **515**: 674 (2006).
- [12] K. Onozuka, B. Ding, Y. Tsuge, T. Naka, M. Yamazaki, S. Sugi, S. Ohno, M. Yoshikawa, S. Shiratori. *Nanotechnology* **17**, 1026 (2006).
- [13] J. Xiang, Y. Masuda, K. Koumoto. *Adv. Mater.* **16**(16), 1461 (2004).
- [14] H. Yun, K. Miyazawa, H. Zhou, I. Honma M. Kuwabara. *Adv. Mater.* **13**(18), 1377 (2001).
- [15] Z. Zainal, C.Y. Lee. *J. Sol-Gel Sci. Techn.* **37**, 19 (2006).
- [16] A. Verma, A. Basu, A.K. Bakhshi, S. A. Agnihotry. *Solid State Ionics*, **176**, 2285 (2005).
- [17] M. Bockmeyer, P. Lobmann. *Chem. Mater.* **18**, 4478 (2006).
- [18] J. N. Harta, D. Menzies, Y.B. Cheng, G.P. Simon L. Spiccia. *Sol. Ene. Mat. Sol. C.* **91**, 6 (2007).
- [19] G. J. Wilson, A.S. Matijasevich, D.G. Mitchell, J.C. Schulz, G.D. Wall. *Langmuir* **22**, 2016 (2006).
- [20] O. Carp, C.L. Huisman, A. Reller, *Prog. Solid State Chem.* **32**, 33 (2004).
- [21] A. Jaroenworarluck, T. Panyathanmaporn, B. Soontornworajit. *Surf. Interface Anal.* **38**, 765 (2006).
- [22] A. Hagfeldt, M. Gratzel. *Chem. Rev.* **95**, 49 (1995).
- [23] K. M. Reddy, S.V. Manorama, A.R. Reddy. *Mater. Chem. Phy.* **78**, 239 (2002).

*Corresponding author: hmyang@mail.csu.edu.cn